


## THE MARINE RESERVOIR EFFECT: A CASE STUDY OF ARCHAEOLOGICAL SITES AT GUANABARA BAY, RIO DE JANEIRO, BRAZIL

Ronaldo Janvrot Vivone<sup>1</sup> • Zenildo Lara de Carvalho<sup>1</sup> • Ricardo Tadeu Lopes<sup>2</sup> • Roberto Ventura dos Santos<sup>3</sup> • José Marcus Godoy<sup>4\*</sup> 

<sup>1</sup>Divisão de Radioproteção Ambiental e Ocupacional, Instituto de Radioproteção e Dosimetria, Rio de Janeiro, RJ, 22783-127, Brazil

<sup>2</sup>Programa de Engenharia Nuclear, COPPE, Universidade Federal do Rio de Janeiro, Cidade Universitária, Rio de Janeiro, RJ, 21945-970, Brazil

<sup>3</sup>Universidade de Brasília, Instituto de Geociências, Campus Universitário Darcy Ribeiro CEP 70910-900 Brasília, DF, Brazil

<sup>4</sup>Departamento de Química, Pontifícia Universidade Católica do Rio de Janeiro, Rio de Janeiro-RJ, 22453-900, Brazil

**ABSTRACT.** This study applied, radiocarbon dating to charcoal and mollusk samples from Sernambetiba and Amourins archaeological sites in the Northeast region of Guanabara Bay, in the state of Rio de Janeiro, Brazil, to assess the marine radiocarbon reservoir effect (MRE) of this area, being applied for the correction of the marine samples ages. The results for this estuarine system were  $\Delta R = -87 \pm 90$  <sup>14</sup>C yr and  $\Delta R = -244 \pm 70$  <sup>14</sup>C yr for  $3970 \pm 70$  <sup>14</sup>C yr BP and  $2357 \pm 60$  <sup>14</sup>C yr BP, respectively. Based on these findings, calibrated <sup>14</sup>C ages were calculated for Sernambetiba and Amourins shell mound sites surrounding the bay. Marine samples from the Guapi site were analyzed and only their radiocarbon ages presented because there were no paired terrestrial samples for the MRE assessment. These results are coherent with previously published values also derived from archaeological samples for the Rio de Janeiro state coastal region and contribute to the interpretation of human occupation of the region during the Holocene.

**KEYWORDS:** Guanabara Bay, reservoir effect, shell mounds.

### INTRODUCTION

Reliable radiocarbon dating results require knowledge about the origin and distribution of <sup>14</sup>C in different environmental compartments. In an aquatic environment, the dissolution of carbon dioxide through the air/ocean interface is responsible for the presence of radiocarbon in the oceans. This process is not uniform across the oceans, and in addition, marine currents also contribute to variations in <sup>14</sup>C activities at different water samples. Surface waters have <sup>14</sup>C higher activities than deep waters (Alves et al. 2015a, 2018; Sikes et al. 2016).

Because of these factors, it is not possible to directly compare the radiocarbon ages of contemporary terrestrial and marine samples. Marine samples present older radiocarbon ages caused by the uptake of <sup>14</sup>C that has already suffered radioactive decay due to long residence times in deep oceans, comprising the so-called “marine reservoir age R (t)” (Evin et al. 1980; Goodfriend and Stipp 1983; Goslar and Pazdur 1985; Yates 1986). This scenario is even more complex in estuarine environments due to the influence of freshwater intake and ocean dynamics (Goodfriend and Flessa 1997; Ulm 2002). Thus, whenever <sup>14</sup>C measurements are performed on sea-influenced material, a correction is necessary to compare with terrestrial samples, but because of complexities in ocean circulation the actual correction varies with location. This regional difference from the average global marine reservoir correction is designated  $\Delta R$  (Stuiver and Braziunas 1993).

The reservoir effect ( $\Delta R$ ) parameter measures the variation in marine reservoir age between regions. It is the difference of local marine reservoir age in relation to the globally averaged mixed-layer reservoir age ( $R^{\text{global}}$ ), which exhibits a mean value of around (500±60) during the last 11.6 kyr (Fischer and Olsen 2021). Besides being an important correction for

\*Corresponding author. Email: [jmgodoy@puc-rio.br](mailto:jmgodoy@puc-rio.br)

marine sample  $^{14}\text{C}$  ages (Stuiver et al. 1998), the  $\Delta R$  can also be employed as an upwelling effect indicator. High positive values can be correlated to strong upwelling events, whereas low or negative  $\Delta R$  values correspond to weak or non-existent upwelling events (Diffenbaugh et al. 2003). But the upwelling is not the only reason for these differences, we need take into account species-specific effects, habitat and/or substrate too, which can impact local  $\Delta R$  determinations (Lindauer et al. 2017; Petchey 2020).

Coastal locations are highly influenced by hydrographic conditions, environmental factors and sources of terrestrial carbon which can be expected to modify the local reservoir age  $R(t)$  (Lougheed et al. 2013). Numerous research around the world, for example, in Atlantic Iberia (Soares 2010), the Baltic Sea (Lougheed et al. 2013), and southern and eastern South Africa (Maboya et al. 2018) indicates the variability of  $\Delta R$  in coastal waters.

In freshwater rivers and lakes, there is a similar effect to the marine reservoir effect on radiocarbon dates. It is known as the freshwater reservoir effect (FRE). In these systems, carbon comes from two sources:  $\text{CO}_2$  from the atmosphere and dissolved inorganic carbon (DIC) from the groundwater (Wood et al. 2013), being those arising from the dissolution of carbonate minerals is the largest source of “old” carbon in freshwater (Svyatko et al. 2015).

One of the ways to determine the marine reservoir age  $R(t)$  is by dating paired marine and terrestrial samples from contemporary archaeological contexts (Head et al. 1983; Dettman et al. 2015; Hadden and Cherkinsky 2015; Latorre et al. 2017). The local reservoir age  $R(t)$  is determined by the difference between these ages, and it is expressed for a specific location and calendar age  $t$ . The regional corrections of the  $R(t)$  are reported as  $\Delta R$  values, i.e.,

$$\Delta R^{\text{location}}(t) = R^{\text{location}}(t) - R^{\text{Global Av}}(t)$$

Once calculated,  $\Delta R$  can be applied to to the marine calibration curve (Marine20, Heaton et al. 2020) to calibration of marine  $^{14}\text{C}$  dates. Despite its huge extension, few studies concerning the marine reservoir effect for the Brazilian coast are available (Alves et al. 2015a, 2015b; Carvalho et al. 2015; Macario et al. 2015, 2016).

Shell mounds are the most recognized and studied archeological hill-shaped sites in Brazil, and the object of intense research by Brazilian archeology (Gaspar et al. 2011, 2013, 2014; Klokler 2014; Klokler et al. 2018). These mounds were built by fishers and collectors who settled throughout coastal, estuarine and riverine areas, in islands, lagoons, coves, peninsulas, salt marshes, as well as some river courses. They comprise small or large elevations, which in some regions may reach over 70 m high and 500 m long, defined as often stratified deposits of shells, fish bones, lithic and bone artifacts and charcoal, which have been interpreted as funerary spaces (Bianchini et al. 2011), due to the huge concentrations of human burials and the absence of domestic areas (Gaspar 1991; Barbosa 2007). In the last decade, research carried out in the states of São Paulo and Rio de Janeiro has confirmed the function of these sites as cemeteries, following the identification of funeral areas, where burial concentrations are located (Gaspar et al. 2013).

In the present study,  $R(t)$  values obtained from paired shell (marine) and charcoal fragment (terrestrial) samples from the Sernambetiba and Amourins shell mounds at Guanabara Bay are reported (Figure 1). Radiocarbon ages were obtained from marine samples from the Guapi site, located near the Amourins site (Figure 1).  $\Delta R$  value was determined by

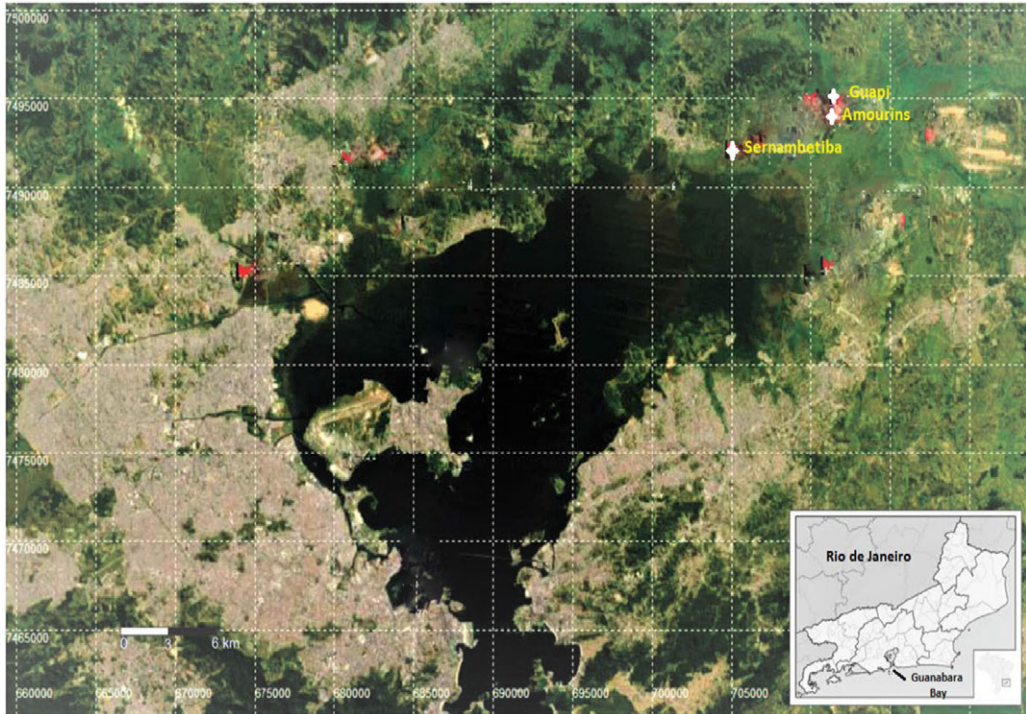


Figure 1 Map displaying the location of the Sernambetiba, Amourins, and Guapi shell mounds near Guanabara Bay.

subtracting the local reservoir age  $R(t)$  value from the globally average mixed layer reservoir age  $R^{\text{global}}$ . Based on the obtained  $\Delta R$  results, calibrated  $^{14}\text{C}$  ages were calculated for the two investigated shell mound sites. The research area is located in the northern portion of the wide sedimentary plain of Guanabara Bay and covers about 7000 km<sup>2</sup>. In this location, twenty shell mound sites are known and registered by the University of Rio de Janeiro National Museum (MN/UFRJ).

According to Amador (1997), the surrounding Guanabara Bay region attracted human occupation, due to the availability of a wide variety of marine foods, such as fish, crustaceans, mollusks, and seaweed, among others, as well as terrestrial foods such as fruits, mammals and reptiles. In addition, freshwater availability from rivers that flow into the Guanabara Bay and forests used to obtain wood material is also noteworthy.

As explained by Amador (1997), around 18,000 cal BP, during the last glacial maximum, the sea level was about 130 m below its current level, maintaining the local coastline tens of kilometers outward compared to the current margins. Guanabara Bay displayed river features during this period, comprising the Paleo-Rio-Guanabara. From 18,000 cal BP, due to gradual global warming and progressive melting of the polar ice caps at high latitudes, several transgressive events took place, partially interrupted by minor regressions and coastline stabilization, followed, a rapid rise in sea level. At about 7948–7598 cal BP, the sea level was 0.5 m below its current level, which was first reached in the Holocene around 7500 cal BP. The maximum level of 3.0 m above the current level was reached between 4787 and 4104 cal BP (Castro et al. 2021). The sea then advanced, reaching the base of the

Serra do Mar Mountain Range and areas which are now located 30 km distant from the coast. At around 4500 cal BP, the sea level began its retreat, until reaching the current level.

At that time, restingas and lagoons were present, local mangroves expanded and dunes, marshes and salt marshes were formed, progressively reducing the surface of the bay until reaching modern settings (Castro et al. 2014). Mangroves exhibited rapid expansion, mainly in the Macao, Guapi-Açu and Guaxindiba river basins, all surrounding Guabanara Bay, and in the basins of other rivers that flow into the area (Amador 1997).

Several shell mound records are noted for the surrounding Guanabara Bay region. About 20 are situated in the Northeastern portion of this area, indicating that the region was densely occupied by ancient groups. Due to the small average distance between settlements (approximately 6 km) and some concomitant dates available in the literature, routine contact between groups can be inferred (Souza et al. 2012; Gaspar et al. 2013; Bianchini 2015; Klokler et al. 2018).

## MATERIAL AND METHODS

### Samples

Samples from the Sernambetiba (16 mollusk shells, *Anomalocardia brasiliensis* and *Lucina pectinata*, and 3 charcoal fragments), Amourins (7 mollusk shells, *Lucina pectinata*, and 3 charcoal fragments), and Guapi (20 *Ostrea* shells) shell mounds were investigated (Figure 1). All samples were obtained from the Federal University of Rio de Janeiro National Museum (MN/UFRJ) archaeological collection. Due to the fire that destroyed the National Museum on 9/2/2018, some of these samples became unique, in particular, those from the Amourins shell mound, whose archaeological site is not well preserved (Gaspar et al. 2013). Figure 2 presents the study region located on the southeastern Brazilian coast and other regions studied by different authors.

The Amourins site was reviewed by Gaspar et al. (2013) and has an age of about 4000 years. Five graves have been identified at Amourins and how they were built was described by Berredo et al. (2020). To seal the graves, there is a sequence of three layers built from ashes, charcoal pieces, fish bones and shells, mainly, *Lucina* (*Lucina pectinata*). Four *Lucina pectinata* shells and charcoal samples came from the seal of the graves identified at the profile 30–35, at a depth of about 1.30 m (Gaspar et al. 2013).

The Sernambetiba site is much younger than Amourins, circa 2000 years (Bianchini 2015). It is composed, in fact, by several sub-hills, each one containing several graves. According to this author, at the Sernambetiba site there is three excavation areas, named locus, and the actual samples came from locus 2 and 3. As a result of how this sambaqui was built and operated, there is not a large time difference according to the sample stratigraphy. Bianchini (2015) has observed charcoal samples with the same age (circa 1900 years) at the surface (0.30 m) and at 5.00 m depth. *Anomalocardia brasiliensis* is the predominant specie but lucinas are present on the top layer that covers the structure.

The Guapi site is the oldest of these three (5000 years) and less studied than Amourins and Sernambetiba, the observed references are internal Nacional Museum report and a M.Sc. dissertation (Pinto 2009; Borges 2015).

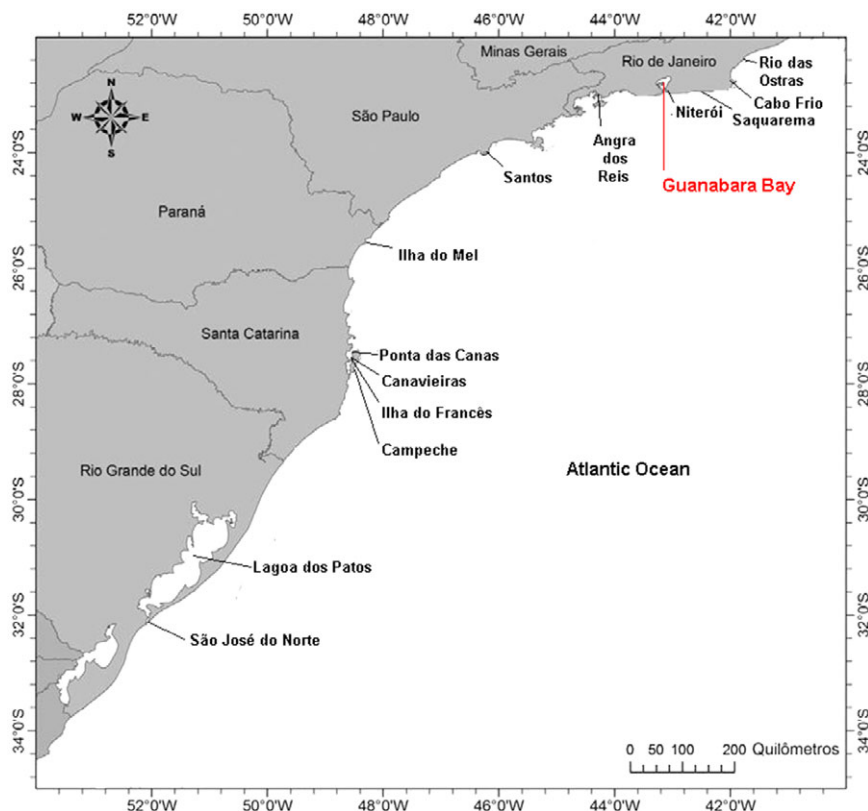


Figure 2 Study region located on the southeastern Brazilian coast (red) and regions studied by other authors (black). (Please see online version for color figure.)

### Radiocarbon Dating

All samples were treated according to Pessenda and Camargo (1991) and dated at the  $^{14}\text{C}$  Laboratory, located at the Radioprotection and Dosimetry Institute, belonging to the Brazilian National Nuclear Energy Commission (IRD/CNEN). Dating was carried out via the benzene synthesis methodology and  $^{14}\text{C}$  activities were determined by liquid scintillation spectrometry. International Atomic Energy Agency carbonate reference standards (IAEA C-2;  $\text{pMC} = 23.05$ ;  $\delta^{13}\text{C} = -25.5\text{‰}$ ), wood (IAEA C-5;  $\text{pMC} = 41.14$ ;  $\delta^{13}\text{C} = -8.3\text{‰}$ ), and marble samples were also submitted to the same procedure (Pessenda and Camargo 1991; Beramendi-Orosco et al. 2006; Bronić et al. 2009; Baydoun et al. 2014).

The samples (40 g of shell and 10 g of charcoal) were pretreated to eliminate potential interferences and to separate the carbon phase of interest. Contamination may originate from sample preparation steps, such as collection and handling, adhering to the samples, or through carbon exchanges. Complete shells were physically pretreated by scraping to remove adhered materials using spatulas, brushes, and tweezers, and chemically by immersion in 4% hydrochloric acid followed by three successive washings with deionized water. Charcoal fragments were treated by the acid-alkaline-acid (AAA) method. This method consisted of treating samples with  $1 \text{ mol L}^{-1}$  hydrochloric acid (HCl) at  $50^\circ\text{C}$  for 4 hr,  $0.1 \text{ mol L}^{-1}$  sodium hydroxide (NaOH) at  $50^\circ\text{C}$  for 4 hr to remove soluble humic acids,

and 1 mol L<sup>-1</sup> HCl at 50°C for 4 hr. Samples were neutralized by washing with distilled water after each acid and alkali wash (Pessenda and Camargo 1991). All the samples were dried at 60°C for 24 hr and ground.

The benzene synthesis system concentrates 92% of the carbon present in samples into this organic molecule. The conversion, which takes place in a closed system under vacuum (TASK benzene synthesizer, Athens, Georgia, USA) initially converts all sample carbon into carbon dioxide. In the case of shell samples, gas formation occurs through the slow addition of 1:1 phosphoric acid, while gas formation occurs through the combustion in a closed system (Parr pump) pressurized with oxygen to a pressure of 200 psi for the charcoal fragments samples. Subsequently, lithium carbide is formed by reacting the carbon dioxide with molten lithium at 850°C and acetylene is formed by reacting lithium carbide with water. In the last step, the acetylene is trimerized by catalysis with vanadium pentoxide, producing benzene.

The synthesized benzene was immediately transferred to a 7 mL vial and mixed with a 0.5 mL scintillation solution containing 43.75 g PPO (2,5-diphenyloxazole) and 2.59 g POPOP [1-4,bis-2-(5-Phenylloxazolyl)-benzene] for measurement. The samples and standards were measured for 24 hours applying a low-level liquid Perkin-Elmer Quantulus 1220 scintillation counter. The counting efficiency for 100 pMC, based on both IAEA <sup>14</sup>C certified reference materials, was 10.72 (0.18) counts per gram carbon and the background was 1.0 count per minute. The δ<sup>13</sup>C values were determined by IRMS at the Stable Isotopes Laboratory, in the University of Brasília Geosciences Institute.

Ages were calculated according to Stuiver and Polach (1977) and correspond to conventional radiocarbon ages. Marine reservoir age R(t) was calculated by the difference between the radiocarbon ages of paired marine and terrestrial samples nearby and in the same layer from the archaeological site. ΔR value was determined by subtracting the local reservoir age R(t) value from the globally average mixed layer reservoir age R<sup>global</sup>.

The radiocarbon ages uncertainties (k=2) comprise expanded propagated uncertainties, including reproducibility, calibration, sample, and blank counting uncertainties. Ages calibration was performed using the OxCal version 4.4 software (Bronk Ramsey 2009). Calibrated ages of the marine samples were obtained using Marine20 curve (Heaton et al. 2020) with application of a local reservoir adjustment, while SHCal20 curve was used for the charcoal samples (Hogg et al. 2020). The applied equations for the radiocarbon ages and the reservoir effect, together with the uncertainty calculation, are presented as Supplementary Material.

## RESULTS AND DISCUSSION

### Radiocarbon Ages and the Reservoir Effect

The obtained radiocarbon and calibrated ages for the Sernambetiba and Amourins mounds are presented in Tables 1–2. Radiocarbon ages for Guapi shell mound are presented in Table 3.

Samples from the Sernambetiba site presented a very narrow age range for charcoal fragments (2480–2280 <sup>14</sup>C BP). The data reveal a mean value of 2586 <sup>14</sup>C BP and an error of the mean of 40 years for *Anomalocardia* shells, and a mean value of 2357 <sup>14</sup>C BP and an error of the mean of 60 <sup>14</sup>C yr for charcoal fragments, resulting in a marine reservoir age of 229 ± 72 <sup>14</sup>C yr. The

Table 1 Sernambetiba shell mound: shell and charcoal sample radiocarbon and calibrated ages and their respective  $\delta^{13}\text{C}$  values.

Site	Lab code	Material	MN/UFRJ code	$\delta^{13}\text{C}$ (‰)	$^{14}\text{C}$ age (BP)	cal BP (2 $\sigma$ )
Sernambetiba	IRD-014	<i>Lucina</i>	NP 30	-1.8	2380 $\pm$ 70	2366–1880
Sernambetiba	IRD-015	<i>Lucina</i>	NP 32	-1.0	2600 $\pm$ 50	2672–2206
Sernambetiba	IRD-018	<i>Anomalocardia</i>	NP 87	-1.0	2550 $\pm$ 50	2610–2126
Sernambetiba	IRD-019	<i>Anomalocardia</i>	NP 88	-0.4	2620 $\pm$ 50	2694–2246
Sernambetiba	IRD-029	<i>Anomalocardia</i>	NP 1003	-0.9	2440 $\pm$ 60	2459–1972
Sernambetiba	IRD-030	<i>Anomalocardia</i>	NP 1004	-1.0	2530 $\pm$ 50	2582–2102
Sernambetiba	IRD-031	<i>Anomalocardia</i>	NP 1059	-1.9	2500 $\pm$ 60	2545–2033
Sernambetiba	IRD-034	<i>Anomalocardia</i>	NP 1061	-1.6	2870 $\pm$ 60	2962–2501
Sernambetiba	IRD-036	<i>Anomalocardia</i>	NP 1062	-1.0	2870 $\pm$ 70	2991–2478
Sernambetiba	IRD-037	<i>Anomalocardia</i>	NP 1077	-1.0	2800 $\pm$ 90	2916–2357
Sernambetiba	IRD-038	<i>Anomalocardia</i>	NP 1077	-2.6	2400 $\pm$ 70	2399–1904
Sernambetiba	IRD-039	<i>Anomalocardia</i>	NP 1078	-0.9	2680 $\pm$ 60	2732–2313
Sernambetiba	IRD-044	<i>Anomalocardia</i>	6-sep-04	-0.5	2400 $\pm$ 50	2353–1936
Sernambetiba	IRD-045	<i>Anomalocardia</i>	4-sep-07	-0.2	2560 $\pm$ 50	2637–2143
Sernambetiba	IRD-046	<i>Anomalocardia</i>	3-sep-09	-0.4	2400 $\pm$ 60	2370–1919
Sernambetiba	IRD-035	<i>Lucina</i>	1-sep-13	-0.1	2830 $\pm$ 60	2926–2453
				<b>Mean*</b>	<b>2586 <math>\pm</math> 40</b>	<b>2652–2189</b>
Sernambetiba	IRD-040	Charcoal	NP 63	-25.0	2310 $\pm$ 70	2490–2091
Sernambetiba	IRD-041	Charcoal	5-sep-07	-25.0	2280 $\pm$ 55	2350–2109
Sernambetiba	IRD-042	Charcoal	2-sep-13	-25.0	2480 $\pm$ 50	2710–2355
				<b>Mean</b>	<b>2357 <math>\pm</math> 60</b>	<b>2685–2139</b>

\*For *Anomalocardia*.

Table 2 Amourins shell mound: shell and charcoal sample radiocarbon and calibrated ages and their respective  $\delta^{13}\text{C}$  values.

Site	Lab code	Material	MN/UFRJ code	$\delta^{13}\text{C}$ (‰)	$^{14}\text{C}$ age (BP)	cal BP (2 $\sigma$ )
Amourins	IRD-066	<i>Lucina pectinata</i>	NT 68	-3.0	4240 $\pm$ 80	4604–3929
Amourins	IRD-067	<i>Lucina pectinata</i>	NT 181	-2.4	4270 $\pm$ 60	4607–3997
Amourins	IRD-068	<i>Lucina pectinata</i>	NT 82	0.1	4610 $\pm$ 60	5026–4435
Amourins	IRD-070	<i>Lucina pectinata</i>	NT 37	-3.3	4410 $\pm$ 60	4805–4212
				<b>Mean</b>	<b>4382 <math>\pm</math> 100</b>	<b>4811–4100</b>
Amourins	IRD-064	<i>Lucina pectinata</i>	NT 63	-3.1	4070 $\pm$ 60	4352–3740
Amourins	IRD-065	<i>Lucina pectinata</i>	NT 98	-3.9	3590 $\pm$ 70	3720–3135
Amourins	IRD-069	<i>Lucina pectinata</i>	NT 72	-8.4	3560 $\pm$ 60	3678–3113
Amourins	IRD-063	Charcoal	NT 123	-25.0	4080 $\pm$ 180	5038–3985
Amourins	IRD-075	Charcoal	Grave 03/C	-25.0	3980 $\pm$ 60	4572–4156
Amourins	IRD-076	Charcoal	Grave 03/C	-25.0	3850 $\pm$ 60	4414–3992
				<b>Mean</b>	<b>3970 <math>\pm</math> 70</b>	<b>4576–4103</b>

Table 3 Guapi shell mound: shell sample radiocarbon ages and their respective  $\delta^{13}\text{C}$  values.

Site	Lab code	Sample	MN/UFRJ Code	$\delta^{13}\text{C}$ (‰)	$^{14}\text{C}$ age (BP)
Guapi	IRD-013	Ostrea	NP 12	-4.6	4730 $\pm$ 60
Guapi	IRD-020	Ostrea	NP 13	-3.0	4640 $\pm$ 60
Guapi	IRD-021	Ostrea	NP 22	-6.9	4910 $\pm$ 70
Guapi	IRD-022	Ostrea	NP 23	-5.5	5220 $\pm$ 70
Guapi	IRD-023	Ostrea	NP 27	-2.4	5270 $\pm$ 80
Guapi	IRD-025	Ostrea	NP 29	-2.9	4920 $\pm$ 80
Guapi	IRD-026	Ostrea	NP 31	-3.0	4950 $\pm$ 60
Guapi	IRD-027	Ostrea	NP 34	-3.0	5490 $\pm$ 70
Guapi	IRD-032	Ostrea	NP 201	-3.8	5080 $\pm$ 100
Guapi	IRD-047	Ostrea	NP 202	-4.2	5270 $\pm$ 60
Guapi	IRD-048	Ostrea	NP 203	-3.4	5370 $\pm$ 60
Guapi	IRD-049	Ostrea	NP 210	-1.7	5430 $\pm$ 60
Guapi	IRD-051	Ostrea	NP 216	-6.0	5060 $\pm$ 60
Guapi	IRD-052	Ostrea	NP 219	-5.6	4720 $\pm$ 60
Guapi	IRD-053	Ostrea	NP 224	-4.9	5200 $\pm$ 90
Guapi	IRD-055	Ostrea	NP 235	-4.1	4590 $\pm$ 60
Guapi	IRD-056	Ostrea	NP 236	-7.0	5040 $\pm$ 100
Guapi	IRD-054	Ostrea	NP 238	-3.6	5080 $\pm$ 70
Guapi	IRD-057	Ostrea	NP 239	-3.6	5060 $\pm$ 90
Guapi	IRD-058	Ostrea	NP 242	-4.84	4610 $\pm$ 100
				<b>Mean</b>	<b>5030 <math>\pm</math> 60</b>



Table 4 Comparison between published marine reservoir effects along the Rio de Janeiro state coast and the present assessment.\*

Local	$\Delta R$ ( $^{14}\text{C}$ yr)	Radiocarbon age ( $^{14}\text{C}$ yr BP)	Reference
Cabo Frio, RJ	$-40 \pm 17$	$563 \pm 17$	Alves et al. (2015a)
Cabo Frio, RJ	$-69 \pm 33$	$1590 \pm 110$	Macario et al. (2016)
Jurujuba, Niterói, RJ	$67 \pm 26$	$670 \pm 26$	Angulo et al. (2005)
Ilha Grande, RJ	$-191 \pm 25$	$420 \pm 25$	Alves et al. (2021)
Copacabana, RJ	$-121 \pm 42$	$483 \pm 42$	Alves et al. (2021)
Rio das Ostras, RJ	$-262 \pm 70$	$3663 \pm 28$	Macario et al. (2015)
Saquarema, RJ	$-177 \pm 74$	$4080 \pm 25$	Carvalho et al. (2015)
Saquarema, RJ	$-235 \pm 68$	$3842 \pm 46$	Alves et al. (2015b)
Guanabara Bay, RJ	$-244 \pm 70$	$2600 \pm 40$	This study
Guanabara Bay, RJ	$-87 \pm 90$	$4320 \pm 80$	This study

\*The values herein from the literature are the adjusted values from calib.org/marine due to the new global marine R.

marine reservoir age was also calculated pairing shell and charcoal fragment samples, obtaining a value of  $256 \pm 37$   $^{14}\text{C}$  yr, although both values were statically equal.

On the other hand, shell samples from the Amourins site presented a broader age range (4610–3560  $^{14}\text{C}$  BP), while charcoal samples presented a narrower age range (4080–3850  $^{14}\text{C}$  BP). Four *Lucina pectinata* shells located near the charcoal samples were used to calculate the marine reservoir age. A mean age value of  $4382 \pm 100$   $^{14}\text{C}$  BP and a mean of  $3970 \pm 70$   $^{14}\text{C}$  BP were obtained to marine and terrestrial samples, respectively. These results provide a marine reservoir age of  $412 \pm 118$   $^{14}\text{C}$  yr. The obtained reservoir age based on shell and charcoal fragment pairing was of  $413 \pm 67$   $^{14}\text{C}$  yr, with both values statically equal.

Comparing the ages of both sites, Amourins corresponds to a period of higher sea level compared to Sernambetiba (Amador 1997) and, therefore, subjected to a lesser estuarine influence. Furthermore, a higher sea level denotes a larger reservoir effect, as observed herein. Applying ( $500 \pm 60$ ) yr as  $R^{\text{Global Av}}$ , for the last 11.6 kyr (Fischer and Olsen 2021), the calculated  $\Delta R$  values were  $-87 \pm 90$  and  $-244 \pm 70$   $^{14}\text{C}$  yr for Amourins and Sernambetiba shell samples, which were used to calibrate marine sample ages for the investigated archaeological sites. Table 4 compared the obtained  $\Delta R$  values to those reported in the literature. All values were calculated based on the MARINE20 curve (Heaton et al. 2020). The values observed herein are consistent with published values for the Rio de Janeiro state coastal region (Alves et al. 2015b; Carvalho et al. 2015; Macario et al. 2015; Macario et al. 2016).

The Guapi shell mound represents a long-lasting site, with radiocarbon ages ranging from 4590–5490  $^{14}\text{C}$  BP. As pointed out by Gaspar et al. (2013) the existence of shell mound sites displaying millennial occupation history reinforce the hypotheses that the shell mound peoples achieved a very large population, supporting the growth of the shell mound itself but also their cultural values. Comparing the shell mound site location (Figure 1) to shell ages, the distance to the actual coastal line follows an age sequence, where the older site (Guapi) is located farther to the actual coastal line than the younger site (Sernambetiba), corroborating seawater level variations throughout the last 12,000 years (Castro et al.

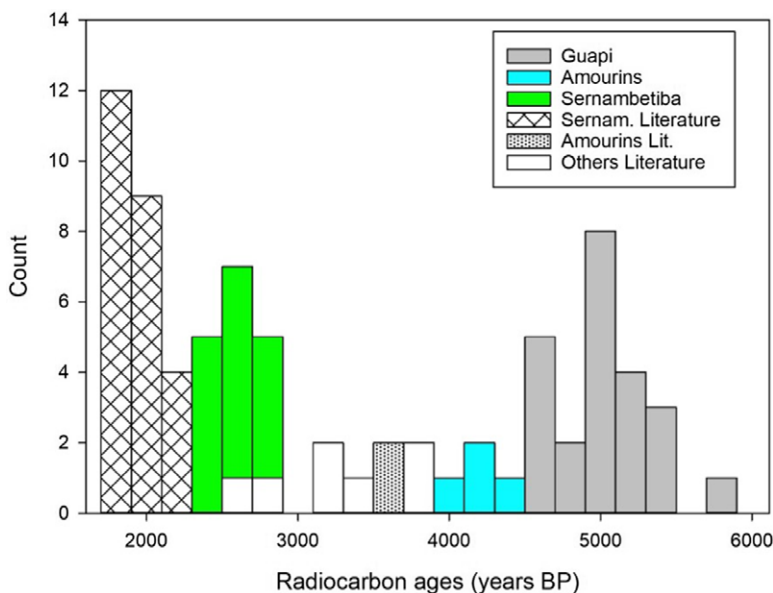


Figure 3 This study and published Guanabara Bay radiocarbon shell mound ages.

2014). Amourins, displaying an intermediate age, is located closer to Guapi than to Sernambetiba, verified by their age difference.

Figure 3 presents the age distribution for the investigated Guanabara Bay shell mounds, including values of this study as well as existing literature data. A continuous existence of shell mound peoples is, thus, verified around Guanabara Bay, lasting, at least, 4000 years, beginning about 6000 years ago and ending circa 1800 years ago when the arrival of more belligerent populations, such as the Tupi-Guarani, led to the end of their civilization (Macario et al. 2014). Although they continuously inhabited this region, as it is a very flat area, these peoples were affected by sea-level changes, moving periodically to avoid long distances to the shoreline.

## CONCLUSIONS

This study aimed to expand knowledge concerning the poorly studied marine reservoir effect and paleoclimatic conditions along the western South Atlantic coast, specifically at Guanabara Bay.  $\Delta R$  values were obtained employing paired shell mound samples from two archaeological sites in this region during the middle to late Holocene. The marine reservoir effects for this estuarine system were  $\Delta R = -87 \pm 90$   $^{14}\text{C}$  yr and  $\Delta R = -244 \pm 70$   $^{14}\text{C}$  yr for  $3970 \pm 70$  yr BP and  $2357 \pm 60$  yr BP, respectively, probably due to the increased influence of fresh water over the period. These new results are coherent with previously published values for the Rio de Janeiro state coastal region.

Samples from the two archaeological sites at Guapimirim (Sernambetiba and Amourins) Rio de Janeiro, were dated using the obtained  $\Delta R$  values, and from one site (Guapi) radiocarbon ages were presented, contributing with the age database concerning shell mounds at Guanabara Bay Region.

## ACKNOWLEDGMENTS

The authors would like to thank Maria Dulce Gaspar and Gina F. Bianchini (Museu Nacional/ Universidade Federal do Rio de Janeiro), who kindly provided the shell mound samples.

## SUPPLEMENTARY MATERIAL

To view supplementary material for this article, please visit <https://doi.org/10.1017/RDC.2022.73>

## REFERENCES

- Alves E, Macario K, Souza R, Pimenta A, Douka K, Oliveira F, Chanca I, Angulo R. 2015a. Radiocarbon reservoir corrections on the Brazilian coast from pre-bomb marine shells. *Quaternary Geochronology* 29:30–35.
- Alves E, Macario K, Souza R, Aguilera O, Goulart AC, Scheel-Ybert R, Bachelet C, Carvalho C, Oliveira F, Douka K. 2015b. Marine reservoir corrections on the southeastern coast of Brazil: paired samples from the Saquarema shell-mound. *Radiocarbon* 57(4):517–525.
- Alves EQ, Macario K, Ascough P, Bronk Ramsey C. 2018. The worldwide marine radiocarbon reservoir effect: definitions, mechanisms, and prospects. *Reviews of Geophysics* 56(1):278–305.
- Alves EQ, Macario KD, Spotorno P, Oliveira FM, Muniz MC, Fallon S, Souza R, Salvador A, Eschner A, Ramsey CB. 2021. Nineteenth-century expeditions and the radiocarbon marine reservoir effect on the Brazilian coast. *Geochimica et Cosmochimica Acta* 297:276–287.
- Amador E. 1997. Baía de Guanabara e ecossistemas periféricos: homem e natureza. Rio de Janeiro. 539 p.
- Angulo RJ, Souza MC, Reimer PJ, Sasaoka SK. 2005. Reservoir effect of the southern and southeastern Brazilian coast. *Radiocarbon* 47:67–73.
- Barbosa M. 2007. A ocupação pré-colonial da região dos lagos, RJ: sistema de assentamento e relações intersociais entre grupos sambaquianos e grupos ceramistas tupinambá da tradição uma [doctoral thesis]. São Paulo: Universidade de São Paulo.
- Baydoun R, Samad O, Aoun M, Nsouli B, Younes G. 2014. Set-up, optimization and first set of samples at the Radiocarbon Laboratory in Lebanon. *Geochronometria* 41(1):87–91.
- Beramendi-Orosco LE, Gonzalez-Hernandez G, Urrutia-Fucugauchi J, Morton-Bermea O. 2006. Radiocarbon Laboratory at the National Autonomous University of Mexico: first set of samples and new <sup>14</sup>C internal reference material. *Radiocarbon* 48(3):485–491.
- Berredo AL, Gaspar MD, Ramos RR, Bianchini GF. 2020. Ritual funerário no sambaqui de Amourins (Guapimirim/RJ): atividades de preparação do terreno para receber o corpo. *Revista de Arqueologia* 33(1):78–97.
- Bianchini G. 2015. Por entre corpos e conchas: prática social e arquitetura de um sambaqui. Doctor Thesis. Universidade Federal do Rio de Janeiro. 170 p.
- Bianchini GF, Gaspar MD, De Blasis P, Scheel-Ybert R. 2011. Processo de formação do sambaqui Jaboticabeira-II: interpretações através da análise estratigráfica de vestígios vegetais carbonizados. *Revista do Museu de Arqueologia e Etnologia, São Paulo* 21:51–69.
- Borges DDS. 2015. Prepare o terreno, vou construir: Estudo do processo de formação do sambaqui do Guapi [unpublished master's thesis]. Museu Nacional, Universidade Federal do Rio de Janeiro, Rio de Janeiro.
- Bronić IK, Horvatinčić N, Barešić J, Obelić B. 2009. Measurement of <sup>14</sup>C activity by liquid scintillation counting. *Applied Radiation and Isotopes* 67(5):800–804.
- Bronk Ramsey C. 2009. Bayesian analysis of radiocarbon dates. *Radiocarbon* 51(1):337–360.
- Carvalho C, Macario K, De Oliveira MI, Oliveira F, Chanca I, Alves E, Souza R, Aguilera O, Douka K. 2015. Potential use of archaeological snail shells for the calculation of local marine reservoir effect. *Radiocarbon* 57(3):459–467.
- Castro JW, Seoane JC, Fernandes D, Cabral CL, da Cunha AM, Malta JV, Miguel LL, de Oliveira CA, de Oliveira PS, de Souza Tamega FT. 2021. Relative sea-level curve during the Holocene in Rio de Janeiro, Southeastern Brazil: a review of the indicators-RSL, altimetric and geochronological data. *Journal of South American Earth Sciences* 10:103619.
- Castro JWA, Suguio K, Cunha AM, Dias FF. 2014. Sea-level fluctuations and coastal evolution in the state of Rio de Janeiro, southeastern Brazil. *Anais da Academia Brasileira de Ciências* 86:671–683.
- Dettman DL, Mitchell DR, Huckleberry G, Foster MS. 2015. <sup>14</sup>C and marine reservoir effect in archaeological samples from the northeast Gulf of California. *Radiocarbon* 57(5):785–793.
- Diffenbaugh NS, Sloan LC, Snyder MA. 2003. Orbital suppression of wind-driven upwelling in the California Current at 6 ka. *Paleoceanography* 18:1051.
- Evin J, Marechal J, Pachiardi C, Puissegur, JJ. 1980. Conditions involved in dating terrestrial shells. *Radiocarbon* 22:545–555.

- Fischer A, Olsen J. 2021. The Nekselø Fish Weir and marine reservoir effect in Neolithization Period Denmark. *Radiocarbon* 63:805–820.
- Gaspar MD. 1991. Aspectos da organização social de pescadores-coletores: região compreendida entre a Ilha Grande e o delta do Paraíba do Sul, Rio de Janeiro [doctoral thesis]. Universidade de São Paulo. 364 p.
- Gaspar M, Klokler DM, Bianchini GF. 2013. Arqueologia estratégica: abordagens para o estudo da totalidade e construção de sítios monticulares. *Boletim do Museu Paraense Emílio Goeldi. Ciências Humanas* 8:517–833.
- Gaspar M, Klokler D, De Blasis P. 2011. Traditional fishing, mollusk gathering, and the shell mound builders of Santa Catarina, Brazil. *Journal of Ethnobiology* 31:188–212.
- Gaspar M, Klokler D, DeBlasis P. 2014. Were sambaqui people buried in the trash? The cultural dynamics of Shell-matrix sites. Albuquerque (NM): University of New Mexico Press. p. 91–100.
- Gaspar M, Klokler D, Sheel-Ybert R, Bianchini GF. 2013. Sambaqui de Amourins: mesmo sítio, perspectivas diferentes. *Arqueologia de um sambaqui 30 anos depois/Amourins sambaqui: same site, different perspectives. Sambaqui archaeology 30 years later. Revista del Museo de Antropología* 6:7–20.
- Goodfriend GA, Flessa KW. 1997. Radiocarbon reservoir ages in the Gulf of California: roles of upwelling and flow from the Colorado River. *Radiocarbon* 39:139–148.
- Goodfriend GA, Stipp JJ. 1983. Limestone and the problem of radiocarbon dating of land-snail shell carbonate. *Geology* 11:575–577.
- Goslar T, Pazdur MF. 1985. Contamination studies on mollusk shell samples. *Radiocarbon* 27:33–42.
- Hadden CS, Cherkinsky A. 2015. <sup>14</sup>C variations in pre-bomb nearshore habitats of the Florida Panhandle, USA. *Radiocarbon* 57(3):469–479.
- Head J, Jones R, Allen J. 1983. Calculation of the “Marine reservoir effect” from the dating of shell-charcoal paired samples from an Aboriginal Midden on Great Glennie Island, Bass Strait. *Australian Archaeology* 12(17):99–112.
- Heaton TJ, Köhler P, Butzin M, Bard E, Reimer RW, Austin WE, Ramsey CB, Grootes PM, Hughen KA, Kromer B, Reimer PJ. 2020. Marine20—the marine radiocarbon age calibration curve (0–55,000 cal BP). *Radiocarbon* 62(4):779–820.
- Hogg AG, Heaton TJ, Hua Q, Palmer JG, Turney CS, Southon J, et al. 2020. SHCal20 Southern Hemisphere calibration, 0–55,000 years cal BP. *Radiocarbon* 62(4):759–778.
- Klokler D. 2014. A ritually constructed shell mound. The cultural dynamics of Shell-matrix sites. Albuquerque (NM): University of New Mexico Press. p. 151–162.
- Klokler D, Gaspar MD, Scheel-Ybert R. 2018. Why clam? Shell mound construction in southern Brazil. *Journal of Archaeological Science: Reports*.
- Latorre C, De Pol-Holz R, Carter C, Santoro C.M. 2017. Using archaeological shell middens as a proxy for past local coastal upwelling in northern Chile. *Quaternary International* 427:128–136.
- Lindauer S, Santos GM, Steinhof A, Yousif E, Phillips C, Jasim SA, Uerpmann HP, Hinderer M. 2017. The local marine reservoir effect at Kalba (UAE) between the Neolithic and Bronze Age: an indicator of sea level and climate changes. *Quaternary Geochronology* 42:105–116.
- Lougheed BC, Filipsson HL, Snowball I. 2013. Large spatial variations in coastal <sup>14</sup>C reservoir age—a case study from the Baltic Sea. *Climate of the Past* 9(3):1015–1128.
- Maboya ML, Meadows ME, Reimer PJ, Backeberg BC, Haberzettl T. 2018. Late Holocene marine radiocarbon reservoir correction for the southern and eastern coasts of South Africa. *Radiocarbon* 60(2):571–582.
- Macario KD, Souza RCCL, Trindade DC, Decco J, Lima, TA, Aguilera OA, Marques NA, Alves EQ, Oliveira FM, Chanca IS, et al. 2014. Chronological model of a Brazilian Holocene shellmound (Sambaqui de Tarioba, Rio de Janeiro, Brazil). *Radiocarbon* 56:489–499.
- Macario KD, Souza RCCL, Aguilera OA, Carvalho C, Oliveira FM, Alves EQ, Chanca IS, Silva EP, Douka K, Decco J, Trindade DC. 2015. Marine reservoir effect on the southeastern coast of Brazil: results from the Tarioba shell mound paired samples. *Journal of Environmental Radioactivity* 143:14–19.
- Macario KD, Alves EQ, Chanca IS, Oliveira FM, Carvalho C, Souza R, Aguilera O, Tenório MC, Rapagnã LC, Douka K, Silva E. 2016. The Usiminas shell mound on the Cabo Frio Island: marine reservoir effect in an upwelling region on the coast of Brazil. *Quaternary Geochronology* 35:36–42.
- Petchev F. 2020. New evidence for a mid-to late-Holocene change in the marine reservoir effect across the South Pacific Gyre. *Radiocarbon* 62(1):127–139.
- Pinto, DC. 2009. Concha sobre concha: construindo sambaquis e a paisagem no Recôncavo da Baía de Guanabara (doctoral dissertation). Dissertação de Mestrado em Arqueologia. Museu Nacional. Universidade Federal do Rio de Janeiro.
- Pessenda LCR, Camargo PB. 1991. Datações radiocarbônicas de amostras de interesse arqueológico e geológico por espectrometria de cintilação líquida de baixa radiação de fundo. *Química Nova* 14:98–103.
- Sikes EL, Cook MS, Guilderson TP. 2016. Reduced deep ocean ventilation in the Southern Pacific

- Ocean during the last glaciation persisted into the deglaciation. *Earth and Planetary Science Letters* 438:130–138.
- Soares AM, Martins JM. 2010. Radiocarbon dating of marine samples from Gulf of Cadiz: the reservoir effect. *Quaternary International* 221(1–2):9–12.
- Souza SM, Liryo A, Bianchini GF, Gaspar MD. 2012. Sambaqui do Amourins: mortos para mounds? *Revista de Arqueologia* 25(2):84–103.
- Stuiver M, Braziunas TF. 1993. Modeling atmospheric  $^{14}\text{C}$  influences and  $^{14}\text{C}$  ages of marine samples to 10,000 BC. *Radiocarbon* 35:137–189.
- Stuiver M, Polach HA. 1977. Discussion: reporting of  $^{14}\text{C}$  data. *Radiocarbon* 19(2):355–363.
- Stuiver M, Reimer PJ, Braziunas TF. 1998. High-precision radiocarbon age calibration for terrestrial and marine samples. *Radiocarbon* 40:1127–1151.
- Svyatko SV, Mertz IV, Reimer PJ. 2015. Freshwater reservoir effect on redating of Eurasian steppe cultures: first results for Eneolithic and Early Bronze Age northeast Kazakhstan. *Radiocarbon* 57(4):625–644.
- Ulm S. 2002. Marine and estuarine reservoir effects in central Queensland, Australia: Determination of  $\Delta R$  values. *Geoarchaeology* 17:319–348.
- Wood RE, Higham TF, Buzilova A, Suvorov A, Heinemeier J, Olsen J. 2013. Freshwater radiocarbon reservoir effects at the burial ground of Minino, northwest Russia. *Radiocarbon* 55(1):163–177.
- Yates T. 1986. Studies of non-marine mollusks for the selection of shell samples for radiocarbon dating. *Radiocarbon* 28:457–463.